Accepted Manuscript

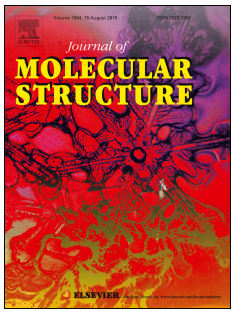

Structure and properties evolution with inorganic and organic acids of a new organo-chlorocadmate compound $(C_6H_{20}N_3)_2[Cd_2Cl_{10}]$: Theoretical approach

Ali Harchani, Cameron L. Carpenter-Warren, Alexandra M.Z. Slawin, Amor Haddad

PII: S0022-2860(19)30544-7

DOI: https://doi.org/10.1016/j.molstruc.2019.04.133

Reference: MOLSTR 26505

To appear in: *Journal of Molecular Structure*

Received Date: 28 January 2019

Revised Date: 29 April 2019

Accepted Date: 30 April 2019

Please cite this article as: A. Harchani, C.L. Carpenter-Warren, A.M.Z. Slawin, A. Haddad, Structure and properties evolution with inorganic and organic acids of a new organo-chlorocadmate compound $(C_6H_{20}N_3)_2[Cd_2Cl_{10}]$: Theoretical approach, *Journal of Molecular Structure* (2019), doi: https://doi.org/10.1016/j.molstruc.2019.04.133.

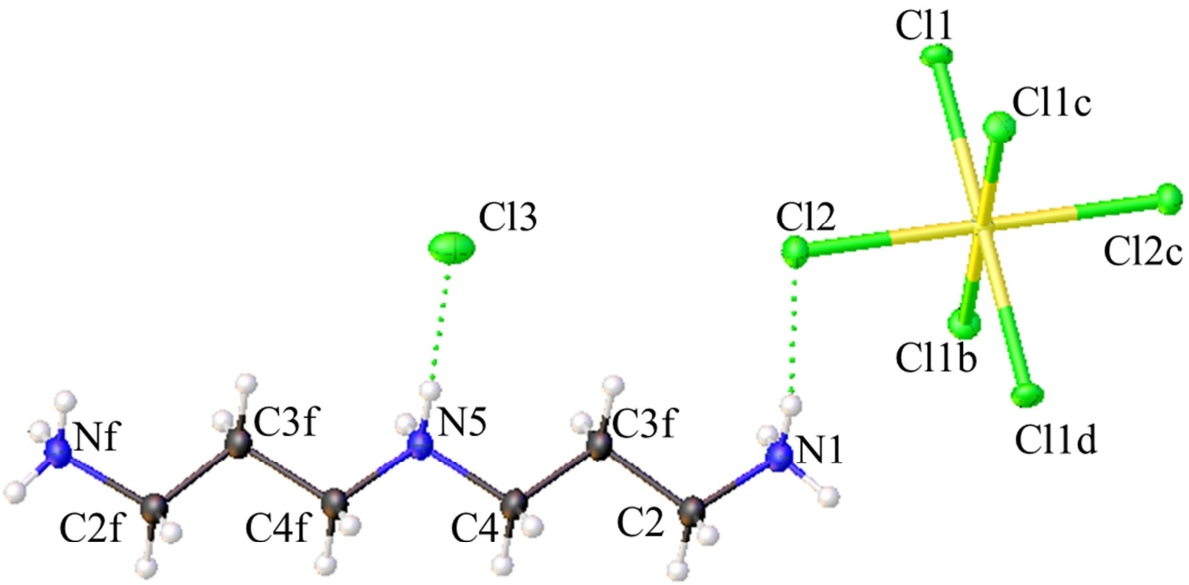

Structure and Properties evolution with inorganic and organic acids of a new organo-chlorocadmate compound $(C_6H_{20}N_3)_2[Cd_2Cl_{10}]$: Theoretical approach

Ali Harchani [a*], Cameron L. Carpenter-Warren [b], Alexandra M. Z. Slawin [b] and Amor Haddad [a]

[a]Laboratoire de Matériaux, Cristallochimie et de Thermodynamique Appliquée. Université de Monastir, Faculté des Sciences Monastir, 5000 Monastir, Tunisia

[b]EaStCHEM, School of Chemistry, University of St Andrews, St Andrews, Fife, KY16 9ST Scotland, UK

e-mail: ali.harchani@gmail.com

Abstract

This work describes the theoretical studies of the reactivity, electrical and thermodynamic properties of a novel organo-chlorocadmate complex $(C_6H_{20}N_3)_2[Cd_2Cl_{10}]$ and its inorganic and organic acid derivatives. The synthesis and crystal structure are described, with the compound crystallizing in the orthorhombic (*Pnma*) space group with unit cell parameters: *a* = 7.25494(11) Å, *b* = 29.3000(5) Å, *c* = 7.33927(13) Å. The semi-empirical calculations reveal that not only are all of the derivatives semiconductors, but also that the inclusion of acids in the structure alter the electrical and thermodynamic properties significantly, demonstrating a systematic and easy method for tuning the materials reactivity along with other desirable properties.

Keywords: Synthesis; Structure; organo-chlorocadmate; acids; Theoretical study;

1. Introduction

In recent years, the chemistry of organo-metal halides has developed rapidly and become very important. These compounds are now applied in a wide range of fields, including catalysis, biochemistry, magnetism and materials science [1-7]. These types of compounds have received so much attention as a result of their exceptionally diverse characteristics.

Organo-metal halides complexes are a very important class and recently several compounds of this type have been synthesized and reported, such as $(C_{12}H_{11}N_3)_2[Cd_2Cl_8]$ [8], $(C_7H_{18}N_2O)_2[Cd_2Cl_8]$ [9], $[(C_{10}H_{10}N_6)(Cd_2Cl_8)_{0.5}].H_2O$ [10], and $[(C_5H_6N_5)_2(CH_2)_3]_2[Cd_2Cl_8(H_2O)_2]\cdot 4H_2O$ [11].

Although many organo-chlorocadmate compounds have been synthesized and characterized, by single-crystal X-ray diffraction, only some of them have been studied theoretically, even though computational analysis has became one of the effective methods to gain informations about the electronic properties, reactivity and thermodynamic properties of this type of compounds. From the small number of papers which report a theoretical studies of organo-chlorocadmates we list the works of Jian et al. [12], Soudani et al. [13], Amamou et al. [14] and Yang et al [15]. which report some theoretical calculations of chlorocadmate compounds.

In the first part of this work, we focus on the synthesis of a new compound $(C_6H_{20}N_3)_2[Cd_2Cl_{10}]$ (**1**), and in the second part we discuss its structure. The third section covers the theoretical properties evolution with inorganic and organic acids of **1**. Here, we focus on the electronic properties by discussing frontier molecular orbitals and the reactivity using molecular modeling and analyzing the electrostatic potential map, along with studying the dipole moment variation and thermodynamic characteristics of the title compound and their derivatives.

2. Experimental details

2.1.Synthesis

For compound **1**, all reagents were purchased from commercial company Sigma-Aldrich and used without further purification. A mixture of $CdCl_2$ (0.50 g, 2.7 mmol), $Na_2MoO_4.2H_2O$ (0.257g, 1.1 mmol) and HCl (1 mL) in H_2O (20 mL) was stirred for 25 minutes. After that, 3,3'iminodipropylamine (0.20 mL, 1.4 mmol) and L-histidine (0.102 g, 0.66 mmol) were added and the mixture was stirred for 20 minutes. After evaporation at room temperature for several days, colorless prisms of **1** had grown. Yield is 0.23 g (35.8%).

2.2.X-ray crystallography

A colorless prism, measuring 0.09 × 0.06 × 0.06 mm^3 was used for single-crystal X-ray diffraction. X-ray diffraction data for compound **1** were collected at 173 K by using a Rigaku FR-X Ultrahigh Brilliance Microfocus RA generator/confocal optics with XtaLAB P200

diffractometer [Mo Kα radiation (λ = 0.71075 Å)]. Intensity data were collected using ω steps accumulating area detector images spanning at least a hemisphere of reciprocal space.

All data were corrected for Lorentz polarization effects. A multiscan absorption correction was applied by using CrystalClear [16]. Structures were solved by dual-space methods (SHELXT [17]) and refined by full-matrix least-squares against F2 (SHELXL-2013[17]). Non-hydrogen atoms were refined anisotropically, and hydrogen atoms were refined using a riding model or freely. All calculations were performed using the CrystalStructure [18] interface. The molecular structure plot was generated using Diamond 3[19] and Mercury program (3.3) [20–22]. Selected crystallographic data are presented in Table 1.

3. Computational details

The program used for theoretical computations is Hyperchem 8.0 [23]. The geometries of the title compound and their derivatives have been optimized using MM+ force fields at the molecular mechanics level of theory. All calculations were carried out in vacuum. The energies and properties were computed using the semi-empirical calculations based on the PM3 model. The PM3 model was parameterized for most transition metals, and it provided good results. The electronic properties, dipole moment, electrostatic potential and thermodynamic properties were calculated based on the vibrational and rotational analysis using PM3 level of Semi-empirical calculations and at 298.15 K and 1.00 atm with spin multiplicity equal to 1, RHF spin pairing and lowest state. The theoretical method which has proven to be one of the most accurate methods for the computation of the electronic structure of solids [24-30].

4. Results and discussion

4.1.Description of the crystal structure

Fig. 1 shows the structure of compound **1**, consisting of a 3,3’iminodipropylamine cation, a chloride anion and one $[CdCl6]^{2-}$ unit.

The structure of **1** consists of $[CdCl6]^{2-}$ repeating units, the anion complex actually is octahedrally coordinated polymer with Cl as a bridging ligand and forms a 2D polymeric structure running parallel to ac-plane and these sheets parallel to one another (Fig. 2). This arrangement of organic cations between sheets makes the structure more stable. The sheets

are also spaced by 3,3'iminodipropylamine ($[C_6H_{20}N_3]^{3+}$) moieties lying perpendicular to the sheets, with Cl^- anions to balance the charge (Fig. 2).

By comparing our structure and the structures of Jian [12], Xia [8], Rong [9], Jin [10] and Raso [11] only the anion of our work forms 2D polymeric structure. The distances Cd–Cl are in the same order. The arrangement of organic cations in published structures and the structure of the title compound slightly resemble.

The Cd–Cl distances are in the range of 2.5831(3) – 2.6332(2) Å and the smallest Cl-Cd-Cl angle is 87.721(8)° (Table S1). The octahedrons $[CdCl_6]$ are linked via corners forming the infinite sheets (Fig. 2 (a)). The Cd···Cd separations within each sheet is 5.1599(11) Å. Adjacent $CdCl_6$ sheets are charge balanced and spaced by the organic 3,3'iminodipropylamine cations, oriented normal to the planes, giving inter sheet Cd···Cd distances of 15.5320 (5) Å (Figs. 2 (b) and 3). The hydrogen atoms on the amine groups of the 3,3'iminodipropylamine cations hydrogen bond to the monocoordinated chlorine atoms on the $CdCl_6$ sheets, with distances of 2.23(2) – 2.390(18) Å (Table 2). The short length of these hydrogen bonds indicates a strong interaction, likely as a result of the high electronegativity of the chlorine atoms, giving compound **1** a great degree of stability.

4.2.Electronic properties

The analysis of Frontier Molecular Orbital (FMO) is an important theoretical method which calculates the energy levels and plays a significant role in the study of molecular reactivity as well as the kinetic stability. The Frontier Molecular Orbital 3D plots of the title compound and its derivatives with inorganic and organic acids are displayed respectively in Figs 4 and 5. Fig. 4 shows the HOMO surfaces to be delocalized over some of the chlorine atoms of the chlorocadmate anion, for the original structure of **1** and for **1** with inorganic acids (**1**).HNO_3, (**1**).H_3PO_4, (**1**).H_2SO_4, (**1**).H_4TiO_4 (**1**).$HBrO_3$, (**1**).H_3AsO_4 and (**1**).H_2SeO_4. The LUMO surfaces are delocalized over one amine group for (**1**), (**1**).HNO_3, (**1**).H_3PO_4, (**1**).H_2SO_4 and (**1**).H_3AsO_4, however for (**1**).H_4TiO_4 and (**1**).H_2SeO_4 the LUMOs lay on the chlorine atoms. For (**1**).$HBrO_3$, the LUMO surfaces are localized arround the bromic acid. Fig. 5 shows that the HOMO surfaces in the organic acid models are situated over chlorine atoms of the chlorocadmate anion. The LUMO surfaces cover one amine group for all models except benzoic acid, where the LUMO surfaces are situated over chlorine atoms of the chlorocadmate.

The energy values of HOMO, LUMO and energy gap are displayed in Figs 4 and 5. It can be seen that energy gap values for (**1**) and its derivatives are between 2 and 4 eV, which allows us to classify these materials as semiconductors. It is worth noting that the energy gap for (**1**) and (**1**).H_2SO_4 are the same and would thus exhibit the same electronic properties. It is also shown that the energy gaps for (**1**).citric acid, (**1**).benzoic acid, (**1**).H_4TiO_4 and (**1**).H_2SeO_4 are higher than the other models, this may be as a result of the size and weight of the molecule. It can be also concluded that the organic acids have more influence on the electronic properties, because generally the energy gap values of **1** with organic acids are higher than energy gap values of **1** with inorganic acids. By comparing with a previous works, mostly the energies are similarly like in the works of Liao et al. [31] which worked well on the semi conductivity of the organo-lead halides.

4.3.Dipole moment

In this part, we discuss the results of the dipole moment calculation and the influence of inorganic and organic acids on the polarity of the title compound structure. It is very interesting to analyze the dipole moment because compound **1** contains chlorine, which has a very strong electronegativity. The dipole moment of the compound **1** and its derivatives were calculated using PM3. The values of (**1**), (**1**).HNO_3, (**1**).H_3PO_4, (**1**).H_2SO_4, (**1**).H_4TiO_4, (**1**).$HBrO_3$, (**1**).H_3AsO_4 and (**1**).H_2SeO_4 are respectively: 59.24, 51.89, 50.7, 61.4, 34.92, 37.97, 57.48, 34.37 Debye. And for (**1**).acetic acid, (**1**).oxalic acid, (**1**).lactic acid, (**1**).malonic acid, (**1**).fumaric acid, (**1**).benzoic acid and (**1**).citric acid, the values are respectively: 37.06, 48.98, 35.15, 41.86, 40.52, 41.47, 38.48 Debye. As can be seen from the results, the dipole moment is very high. This large dipole moment is attributed to the presence of a large number of chlorine atoms and hydrogen bonding interactions between these atoms and amine groups.

Comparing the calculated dipole moment of **1** and their derivatives, (**1**).H_2SO_4 has the largest dipole moment, which explains the use of the sulfuric acid as a solvent in several analyses, because it increases the polarity of molecules. Whereas, the organic acids decrease the polarity of title compound, it can be seen that generally the values of dipole moment of **1** with organic acids are lower than those of **1** and **1** with inorganic acids.

From the dipole moment analysis, it can be concluded that some inorganic acids such as sulfuric acid, increase the ability of the title compound to interact with the surrounding neighboring molecules and suggest a high ionic character. Whereas, the organic acids decrease this properties, because a higher dipole moment indicates a more interactions.

As advantages of dipole moment analysis, providing magnitude of charges and the distance of separation between the charges. Also useful for predicting the nature of the molecules, molecules with zero dipole moment are non polar while the molecule with specific dipole moment are polar in nature, for determining the shape of the molecule: If a molecule has a specific dipole moment then its shape will not be symmetrical, they may be bent or angular and the molecule with zero dipole moment will be symmetrical and has linear shape and also, for comparing the polarities of the molecules, greater the dipole moment value, more will be the polarity and vice versa. These advantages are interesting for indicating the role of acids and comparing the title compound to the derivatives or to previous and possible future analogues.

4.4.Electrostatic potential (EP)

Measuring electrostatic potential is one of the most effective methods of studying the reactivity of molecules, often elucidating the active sites of molecules. The electrostatic potential maps (EPM) of **1** with inorganic acids are illustrated in Fig. 6. The colors in the maps indicate values of the electrostatic potential, with red corresponding to the areas of negative potential and blue corresponding to the areas of positive potential. According to EPMs in the figure, the different values at the surface are clarified by different colors. The red regions (negative potential) are situated generally over the chlorine atoms and the oxygen atoms of inorganic acids. These regions are susceptible to strong electrophilic attack in compound **1** and its derivatives. The areas showing as light green correspond to a low nucleophilic and electrophilic reactivity, which is localized essentially in the middle of the structures. The blue regions are located around the amine groups and correspond to strong nucleophilic reactivity. The electrostatic potential maps (EPM) of **1** with organic acids were illustrated in Fig. 7. The red regions are also located generally over the chlorine atoms and the oxygen atoms of organic acids. In this figure, it can be seen that the blue regions which are susceptible for the nucleophilic attack are smaller than those in Fig. 6. This difference is attributed to the influence of the organic acids which decreases the nucleophilic character. These results are in agreement with those of Dipole moment analysis. By comparing the maps it is found that citric acid has the biggest influence on the reactivity of compound **1** because it has eight oxygen atoms. Generally, it can be concluded that the organic acids have a significant role on the reactivity of the title compound.

4.5.Thermodynamic properties

In this work we report the theoretical thermodynamic properties of compound **1**, to study and discuss the thermodynamic energies and the influence of inorganic and organic acids on these energies. Thermodynamic functions such as zero point energy (ZPE), enthalpy (H^o), heat capacity (C_V) and the entropy (S^o) were calculated at 298.15 K and 1.00 atm at the PM3 level of semi-empirical calculations and are listed in Tables 3 and 4. The enthalpy, heat capacity and the entropy were calculated from 200 to 2000 K on the basis of vibrational analysis and Figures 8-10 show the correlation graphs between thermodynamic functions and temperature.

It can be seen in Tables 3 and 4 that the zero point energy (ZPE) values increases more with the organic acids.

Fig. 8 shows that the enthalpy of the title compound decreases slightly with temperature and the difference in energy is large between the original compound and derivatives, the largest difference being (**1**).Citric acid. The enthalpies of the derivatives also decrease with temperature in the same manor. The energies of (**1**).H_3PO_4, (**1**).H_4TiO_4, and (**1**).H_3AsO_4 were very similar over the whole temperature range, as were (**1**).H_2SO_4 and (**1**).H_2SeO_4. With the organic acids, (**1**).oxalic acid, (**1**).lactic acid, (**1**).malonic acid, (**1**).fumaric acid and (**1**).benzoic acid were all close in value. Globally, acids decrease the enthalpy energies of the title compound.

From Fig. 9, the entropy increases considerably with temperature and the highest energies correspond to (**1**).Arsenic acid and (**1**).Citric acid. It can be seen that all of the acids significantly increase the entropy of the title compound. All derivatives except (1).Arsenic acid and (1).Citric give similar results.

As shown in Fig. 10, the heat capacity increases considerably with temperature inputs of up to 800K, but begins to plateau out between this point and 2000K. As seen for the entropy, both inorganic and organic acids significantly alter the heat capacity of the title compound.

Generally, these results could be used for the further studies on the organo-chlorocadmate compounds. Furthermore, thermodynamic data of this compound and their derivatives are very important to obtain informations about energetic, and reactivity characteristics of these types of compounds. Also, thermodynamic functions, provides several techniques and formulas interesting for the preparation of special materials based on chlorocadmate and acids and taken by chemical industry.

5. Conclusion

In this work the synthesis and the crystal structure determination of a novel organo-chlorocadmate compound, $(C_6H_{20}N_3)_2[Cd_2Cl_{10}]$, have been described. Thorough computational analysis was used to model the HOMO and LUMO surfaces and energies of the title compound, along with its inorganic and organic acid derivatives, showing that all of them can be characterized as semiconductors. The dipole moment and electrostatic potential were also modelled, revealing a significant alteration of the electronic properties upon incorporation of acids into the model. This alteration was most drastic upon incorporation of inorganic acids such as sulfuric acid, which increased the dipole moment of the structure significantly. Under computational investigation of the thermodynamic properties, it was found that the inclusion of acids significantly decreased the enthalpy of the title compound, whilst increasing the entropy and heat capacity, with arsenic and citric acids being the largest deviation all three cases. It can be concluded that the acids which provide the most important properties are the sulfuric and citric acids. So it will be better to use these acids to build the organo-chlorocadmate derivative with the best interesting properties. So mixture of $CdCl_2$, 3,3'iminodipropylamine and one of these two acids leads to the most interesting the organo-chlorocadmate derivative.

Supporting data

CCDC 1828089 contains the supplementary crystallographic data for **1**. These data can be obtained freely via http://www.ccdc.cam.ac.uk/data_request/cif, by e-mailing data_request@ccdc.cam.ac.uk or by contacting directly the Cambridge Crystallographic Data Centre (12 Union Road, Cambridge CB2 1EZ, UK. Fax: +44 1223 336033).

Acknowledgment

This work was supported by the Ministry of Higher Education and Scientific Research of Tunisia.

References

[1] H. Zhao, J. E. Holladay, H. Brown, Z. C. Zhang, Metal Chlorides in Ionic Liquid Solvents Convert Sugars to 5-Hydroxymethylfurfural. *Science* 316 (2007) 1597–1600.

[2] N. Chatani, H. Inoue, T. Ikeda, S. Murai, Ru(II)- and Pt(II)-Catalyzed Cycloisomerization of ω-Aryl-1-alkynes. Generation of Carbocationic Species from Alkynes and Transition Metal Halides and Its Interception by an Aromatic Ring. *J. Org. Chem.* 65 (2000) 4913–4918.

[3] G. Férey, Microporous Solids: From Organically Templated Inorganic Skeletons to Hybrid Frameworks...Ecumenism in Chemistry. *Chem. Mater*. 13 (2001) 3084–3098.

[4] R. J. H. Clark, C. S. Williams, The Far-Infrared Spectra of Metal-Halide Complexes of Pyridine and Related Ligands. *Inorg. Chem*. 4 (1965) 350–357.

[5] J. G. Converse, R. E. McCarley, Chemistry of polynuclear metal halides. VI. Magnetic susceptibility studies of some niobium and tantalum halide cluster derivatives. *Inorg. Chem.* 9 (1970) 1361–1366.

[6] L. Protesescu, S. Yakunin, M. I. Bodnarchuk, F. Krieg, R.Caputo, C. H. Hendon, R. Xi Yang, A.Walsh, M. V. Kovalenko, Nanocrystals of Cesium Lead Halide Perovskites (CsPbX3, X = Cl, Br, and I): Novel Optoelectronic Materials Showing Bright Emission with Wide Color Gamut. *Nano Lett*. 15 (2015) 3692–3696.

[7] T. M. Koh, K. Fu, Y. Fang, S. Chen, T. C. Sum, N. Mathews, S. G. Mhaisalkar, P. P. Boix, T. Baikie, Formamidinium-Containing Metal-Halide: An Alternative Material for Near-IR Absorption Perovskite Solar Cells. *J. Phys. Chem. C* 118 (2014) 16458–16462.

[8] C. K. Xia, Q. Z. Zhang, S. M. Chen, X. He, C. Z. Lu, Bis[2-(3-pyridinio)benzimidazolium] di-l-chloro-bis[trichlorocadmium(II)]. *Acta Cryst*. *C* 61 (2005) m203–m205.

[9] T. Rong, Bis[(2S,4S)-4-(2-hydroxyethyl)-2-methylpiperazine-1,4-diium] di-l-chloridobis[trichloridocadmium(II)]. *Acta Cryst*. E67 (2011) m396.

[10] S. Jin, D. Wang, Syntheses and structural characterization of inorganic–organic hybrid solids of bis-imidazolium chlorocadmate complexes. *J. Coord. Chem*. *63* (2010) 3042–3059.

[11] Á. G. Raso, J. J. Fiol, F. Bádenas, X. Solans, MercèFont-Bardiab Reaction of trimethylene–bisadenine with d10 divalent cations, *Polyhedron* 18 (1999) 765–772.

[12]. F. F. Jian, P. S. Zhao, Q. Xiang, W. Y. Li, One-dimensional Cd metal string complex: Synthesis, structural and thermal properties of $[(HPy)_3(Cd_3Cl_9)]\infty$. *Inorg. Chim. Acta*. 359 (2006) 1473–1477.

[13] S. Soudani, E.Jeanneau, C.Jelsch, F.Lefebvre, C.Ben Nasr, A hirshfeld surface analysis, crystal structure and physicochemical characterization of 1-ethylpiperazinium trichlorocadmate(II). *J. Solid State Sci.* 57 (2016) 49–55.

[14] W. Amamou, H. Feki, N. Chniba-Boudjada, F.Zouari, Synthesis, crystal structure, vibrational properties and theoretical investigation of (N,N-dimethylbenzylammonium)trichlorocadmate(II). *J. Mol. Struct.* 1059 (2014) 169–175.

[15] L. M. Yang, Y. Liu, L. M. Man, J. R. Zhou, X. P. Liu, C. L. Ni, Crystal structure, vibrational spectra, optical properties and density functional theoretical approach of [Bz-4-NH_2Py]$_4$[$CdCl_4$]$_2$·H_2O. *Vib. Spectro*. 93 (2017) 23–28.

[16] CrystalClear-SM Expert v2.1. Rigaku Americas, The Woodlands, Texas, USA, and Rigaku Corporation, Tokyo, Japan, (2015).

[17] G. M. Sheldrick, Crystal structure refinement with SHELXL, *Acta Crystallogr*. A71 (2015) 3-8.

[18] CrystalStructure v4.2. Rigaku Americas, The Woodlands, Texas, USA, and Rigaku Corporation, Tokyo, Japan, (2015).

[19] K. Brandenburg, H. Putz, DIAMOND Version 3. Crystal Impact GbR, Postfach 1251, D-53002 Bonn, Germany, (2005).

[20] C. F. Macrae, P. R. Edgington, P. McCabe, E. Pidcock, G. P. Shields, R. Taylor, M. Towler and J. van de Streek, Mercury: visualization and analysis of crystal structures. *J. Appl. Crystallogr*. 39 (2006) 453–457.

[21] R. Taylor, C. F. Macrae, Rules governing the crystal packing of mono-and dialcohols. *Acta Crystallogr*. B57 (2001) 815–827.

[22] I. J. Bruno, J. C. Cole, P. R. Edgington, M. Kessler, C. F. Macrae, P. McCabe, J. Pearson and R. Taylor, New software for searching the Cambridge Structural Database and visualizing crystal structures. *Acta Crystallogr*. B58 (2002) 389–397.

[23] Hypercube, Inc. Hyperchem, 8.0.6; Hypercube, Inc, USA. (2008).

[24] A. H. Reshak, Spin-polarized Second Harmonic Generation from the Antiferromagnetic CaCoSO Single Crystal. *Scientific Reports* 7 (2017) 46415.

[25] A. H. Reshak, Ab initio study of TaON, an active photocatalyst under visible light irradiation, *Phys. Chem. Chem. Phys.* 16 (2014) 10558–10565.

[26] G. E. Davydyuk, O. Y. Khyzhun, A. H. Reshak, H. Kamarudin, G. L. Myronchuk, S. P. Danylchuk, A. O. Fedorchuk, L. V. Piskach, M. Yu. Mozolyuk and O. V. Parasyuk, Photoelectrical properties and the electronic structure of Tl1−xIn1−xSnxSe2 (x = 0, 0.1, 0.2, 0.25) single crystalline alloys. *Phys. Chem. Chem. Phys.* 15 (2013) 6965–6972.

[27] A. H. Reshak, Y. M. Kogut, A. O. Fedorchuk, O. V. Zamuruyeva, G. L. Myronchuk, O. V. Parasyuk, H. Kamarudin, S. Auluck, K. J. Plucinski and Jiri Bila, Linear, non-linear optical susceptibilities and the hyperpolarizability of the mixed crystals Ag0.5Pb1.75Ge(S1−xSex)4: experiment and theory. *Phys. Chem. Chem. Phys.* 15 (2013) 18979–18986.

[28] A. H. Reshak, D. Stys, S. Auluck and I. V. Kitykd, Dispersion of linear and nonlinear optical susceptibilities and the hyperpolarizability of 3-methyl-4-phenyl-5-(2-pyridyl)-1,2,4-triazole. *Phys. Chem. Chem. Phys*.13 (2011) 2945–2952.

[29] A. H. Reshak, Fe2MnSixGe1−x: influence thermoelectric properties of varying the germanium content. *RSC Adv.4* (2014) 39565–39571.

[30] A. H. Reshak, Thermoelectric properties for AA- and AB-stacking of a carbon nitride polymorph (C3N4). *RSC Adv. 4* (2014) 63137–63142.

[31] W-Q. Liao, Y. Zhang, C-L. Hu, J-G. Mao, H-Y. Ye, P.-F. Li, S. D. Huang, R-G. Xiong, A lead-halide perovskite molecular ferroelectric semiconductor. *Nat. Commun*. 6 (2015) 7338.

Table 1. Crystallographic data and structure refinements

Formula	$(C_6H_{20}N_3)_2[Cd_2Cl_{10}]$ (**1**)
Formula weight (g mol^{-1})	847.84
Temperature (K)	173
Wavelength λ (Å)	0.71075
Space group	Pnma
Unit cell dimensions	
a (Å)	7.25494(11)
b (Å)	29.3000(5)
c (Å)	7.33927(13)
Cell volume (Å^3)	1560.11(5)
Z	2
Absorption coefficient (mm^{-1})	2.23
Crystal size (mm^3)	0.09 × 0.06 × 0.06
Absorption correction	Multi-scan: Tmin = 0.796, Tmax = 0.875
Measured reflections	48589
Independent reflections	1876
Data/restraints/parameters	1876/00/91
Goodness-of-fit	1.29
Weighting scheme	$w = 1/[\sigma^2(F_o^2) + (0.014P)^2 + 0.3544P]$ where $P = (F_o^2 + 2F_c^2)/3$
Final indices R[F^2 > 2σ(F^2)], wR(F^2)	R1 = 0.0115, wR2 = 0.0308
R indices (all data)	R1 = 0.0121, wR2 = 0.0309
$\Delta\rho_{max}$ / $\Delta\rho_{min}$ (e.Å^{-3})	0.29 /-0.52

Table 2. Hydrogen-bond geometry (Å, °) of compound **1**

D—H···*A*	*D*—H	H···*A*	*D*···*A*	*D*—H···*A*
N1—H1*A*···Cl2^{i}	0.854 (17)	2.357 (17)	3.1989 (11)	169.0 (13)
N1—H1*C*···Cl2^{ii}	0.889 (16)	2.375 (16)	3.2430 (11)	165.6 (12)
N1—H1*B*···Cl1	0.853 (19)	2.390 (18)	3.2277 (11)	167.1 (16)
N5—H5*A*···Cl3	0.91 (2)	2.23 (2)	3.1328 (15)	174 (2)
N5—H5*B*···Cl3^{vii}	0.85 (2)	2.27 (2)	3.1208 (14)	174 (2)

Symmetry codes: (ii) *x*-1/2, *y*, -*z*+3/2; (vi) *x*, *y*, *z*-1; (vii) *x*-1/2, -*y*+1/2, -*z*+1/2.

Table 3. Thermodynamic properties at PM3 level of **1** with inorganic acids at 298.15 K and 1.00 atm

Parameters	**Values**							
	(1)	**(1).HNO_3**	**(1).H_3PO_4**	**(1).H_2SO_4**	**(1).H_4TiO_4**	**(1).$HBrO_3$**	**(1).H_3AsO_4**	**(1).H_2SeO_4**
Zero point energy, ZPE (k J mol^{-1})	733.93	797.45	849.10	819.34	854.04	782.14	848.95	831.28
Enthalpy H^o								
Total (k J mol^{-1})	-360311.01	-461566.32	-489816.69	-494276.84	-489461.05	-480226.96	-490151.41	-495025.77
Translational (k J mol^{-1})	-51.80	-52.25	-52.47	-52.47	-52.58	-52.66	-52.74	-52.76
Rotational (k J mol^{-1})	-41.09	-40.59	-41.51	-41.18	-41.63	-41.52	-43.72	-41.53
Vibrational (k J mol^{-1})	683.16	742.54	791.25	760.51	790.80	718.65	780.93	773.19
Heat capacity C_V								
Total (J mol^{-1}K^{-1})	272.38	307.86	334.05	330.71	339.93	320.92	370.02	318.95
Translational (J mol^{-1}K^{-1})	12.5	12.5	12.5	12.5	12.5	12.5	12.5	12.5
Rotational (J mol^{-1}K^{-1})	12.5	12.5	12.5	12.5	12.5	12.5	12.5	12.5
Vibrational (J mol^{-1}K^{-1})	247.38	282.86	309.05	305.71	314.93	295.92	345.02	293.95
Entropy S^o								
Total (J mol^{-1}K^{-1})	655.53	683.16	715.19	715.84	727.08	731.86	782.44	701.66
Translational (J mol^{-1}K^{-1})	186.23	187.7	188.48	188.48	188.85	189.12	189.37	189.43
Rotational (J mol^{-1}K^{-1})	150.30	148.67	151.72	150.60	152.11	151.76	159.11	151.77
Vibrational (J mol^{-1}K^{-1})	319.00	346.79	374.99	376.76	386.12	390.98	433.96	360.46

Table 4. Thermodynamic properties at PM3 level of **1** with organic acids at 298.15 K and 1.00 atm

Parameters	Values							
	(1)	**(1).Acetic acid**	**(1).Oxalic acid**	**(1).Lactic acid**	**(1).Malonic Acid**	**(1).Fumaric acid**	**(1).Benzoic acid**	**(1).Citric acid**
Zero point energy, ZPE (k J mol^{-1})	733.93	886.51	854.16	981.93	935.79	950.76	1035.14	1136.34
Enthalpy H^{o}								
Total (k J mol^{-1})	-360311.01	-445662.94	-499226.51	-488323.01	-513887.24	-525121.28	-505548.53	-639001.4
Translational (k J mol^{-1})	-51.80	-52.23	-52.42	-52.42	-52.51	-52.59	-52.62	-53.02
Rotational (k J mol^{-1})	-41.09	-41.06	-41.64	-41.41	-41.67	-42.06	-41.74	-42.648
Vibrational (k J mol^{-1})	683.16	817.88	786.47	917.53	860.94	894.54	958.61	1054.73
Heat capacity C$_V$								
Total (J mol^{-1}K^{-1})	272.38	337.1	357.39	359.34	355.97	330.15	361.89	431.67
Translational (J mol^{-1}K^{-1})	12.5	12.5	12.5	12.5	12.5	12.5	12.5	12.5
Rotational (J mol^{-1}K^{-1})	12.5	12.5	12.5	12.5	12.5	12.5	12.5	12.5
Vibrational (J mol^{-1}K^{-1})	247.38	312..1	332.39	334.34	330.97	305.15	336.89	406.67
Entropy S^{o}								
Total (J mol^{-1}K^{-1})	655.53	757.92	766.52	750.48	790.79	705.60	796.57	855.20
Translational (J mol^{-1}K^{-1})	186.23	187.66	188.31	188.31	188.61	188.86	188.98	190.32
Rotational (J mol^{-1}K^{-1})	150.30	150.21	152.14	151.39	152.24	153.57	152.49	155.51
Vibrational (J mol^{-1}K^{-1})	319.00	420.05	426.07	410.78	449.94	363.17	455.10	509.37

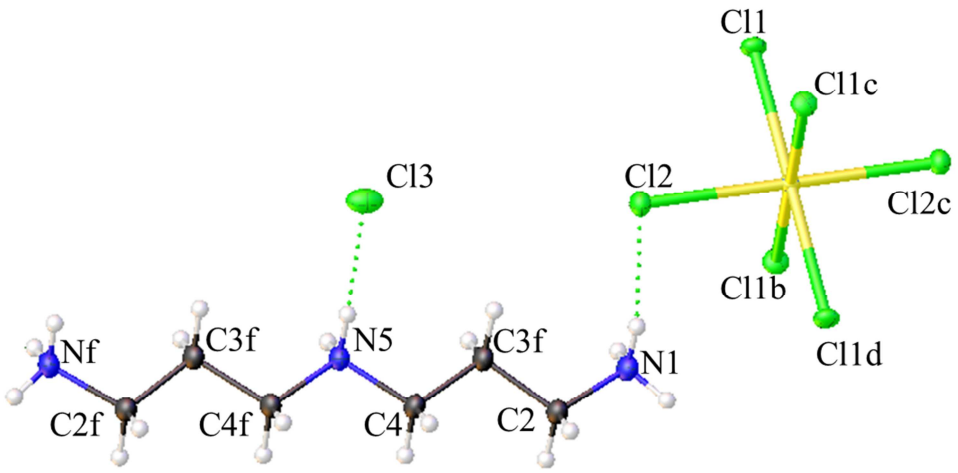

Figure 1. View of structure of compound **1**

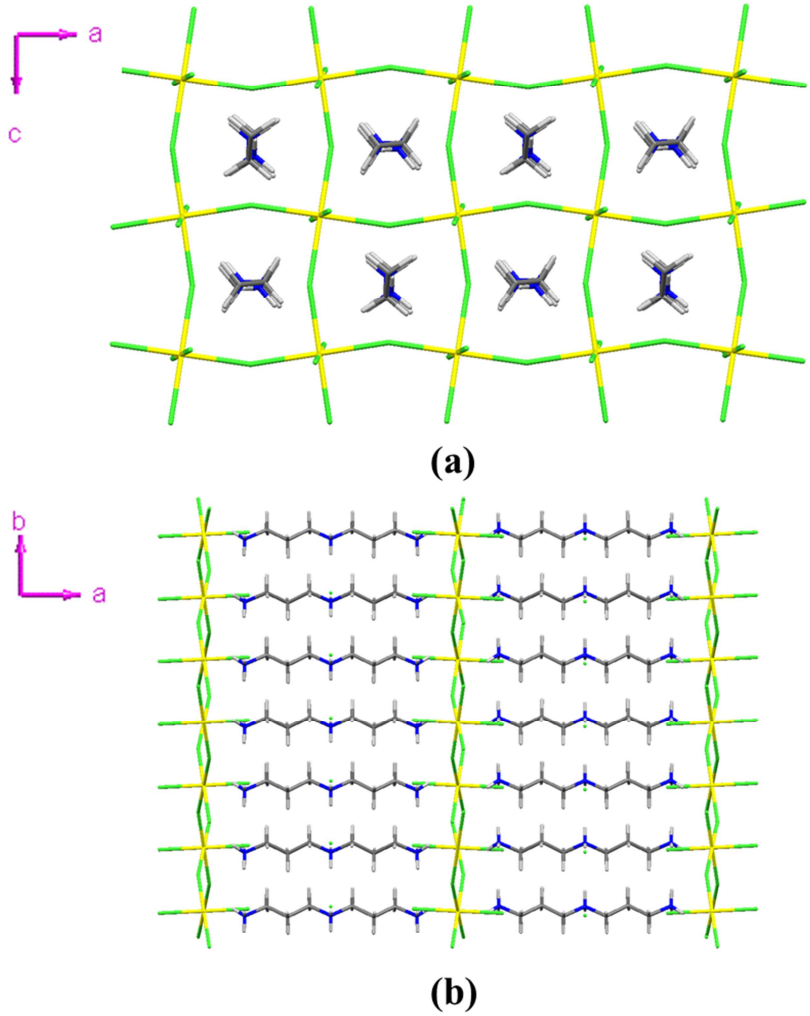

Figure 2. Two views of the arrangement of 1 (a) along *b* and (b) along *c* axes.

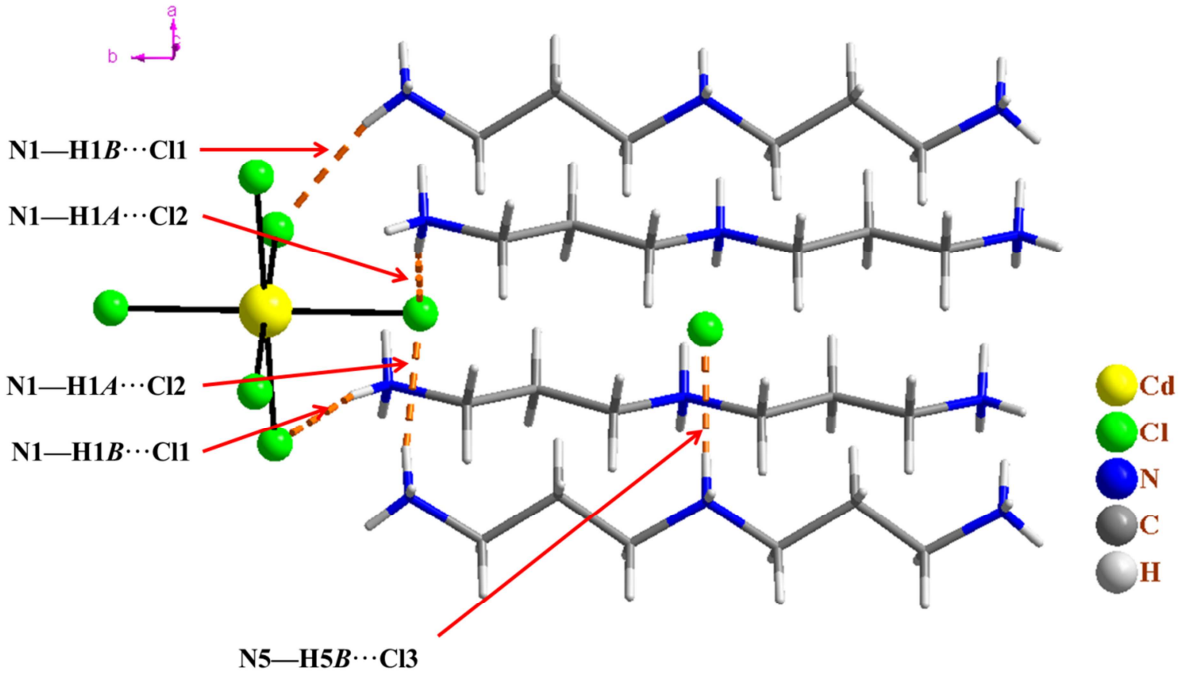

Figure 3. View of the all contacts between anions and cations in compound **1**

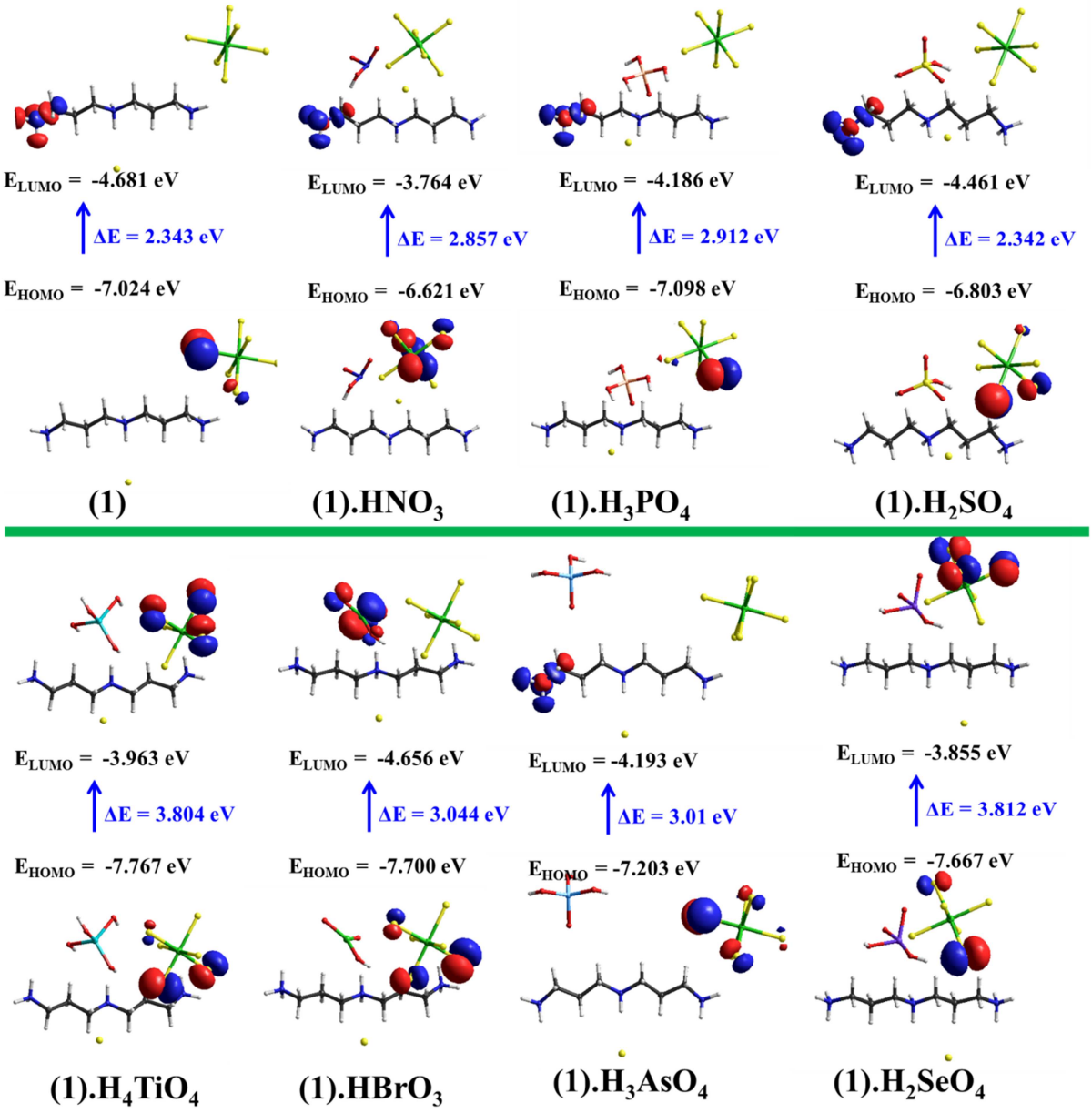

Figure 4. Frontier molecular orbital plots of **1** with inorganic acids

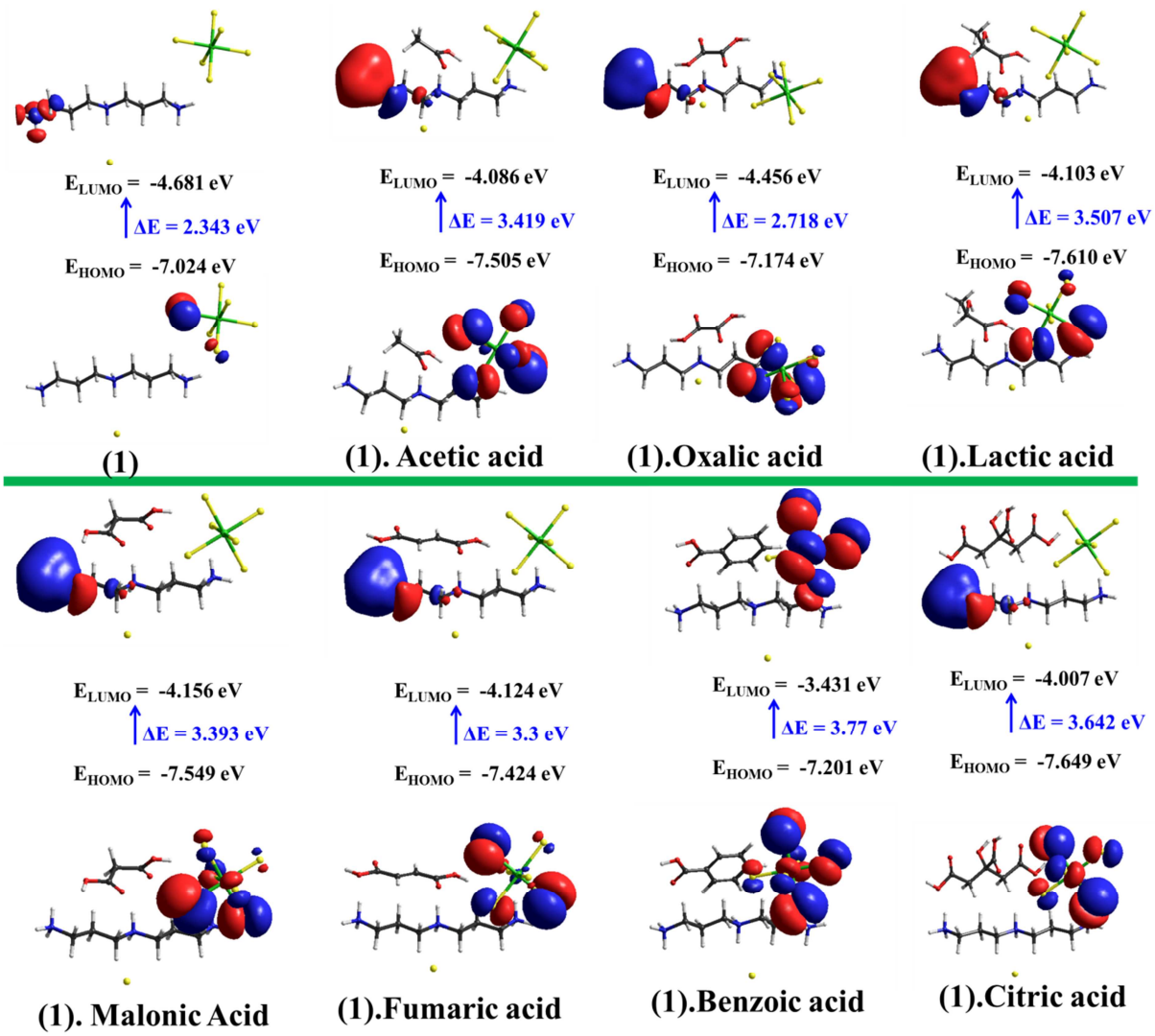

Figure 5. Frontier molecular orbital plots of **1** with organic acids

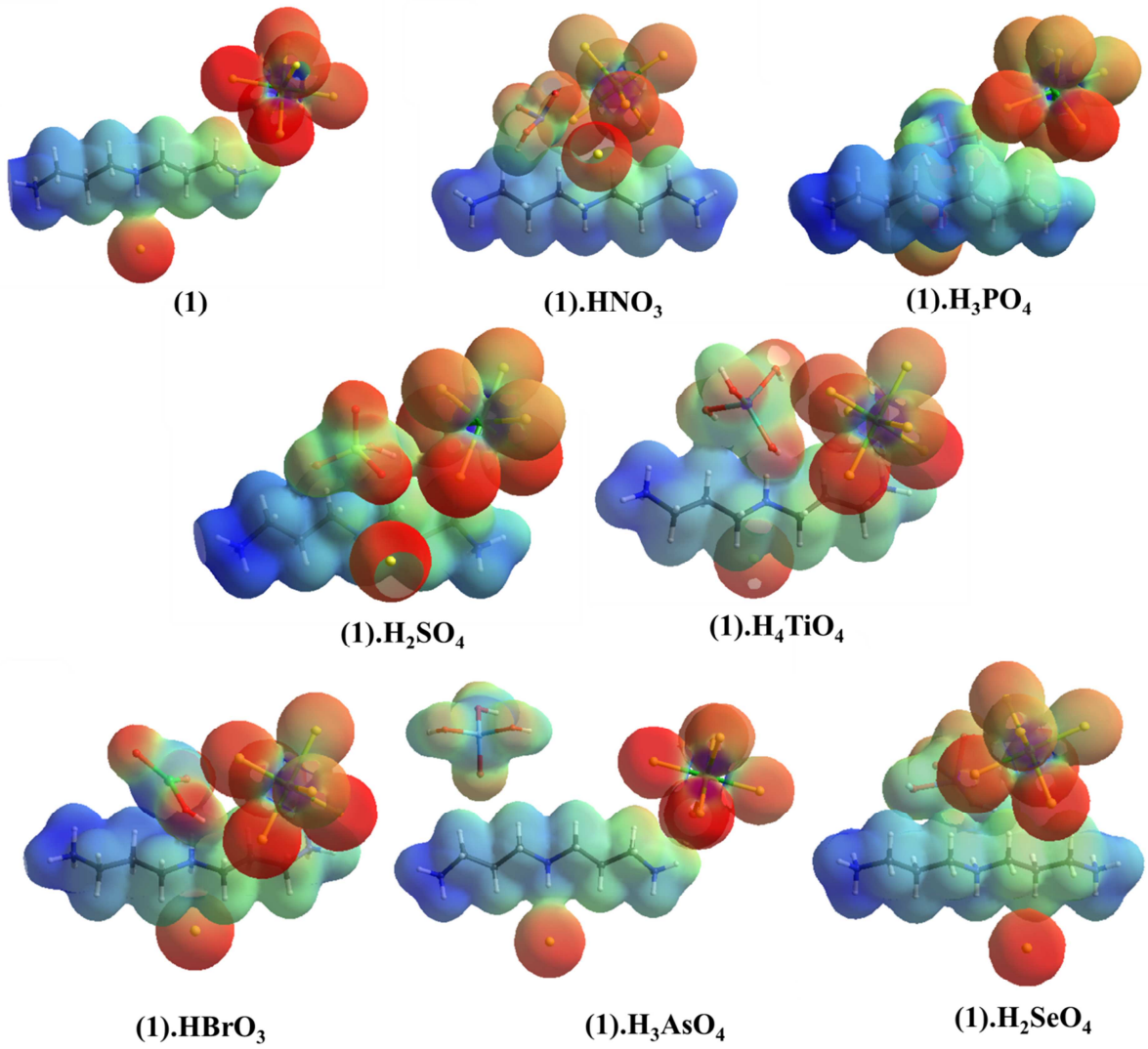

Figure 6 . Electrostatic potential maps (-666—866 kJmol^{-1}) of **1** with inorganic acids

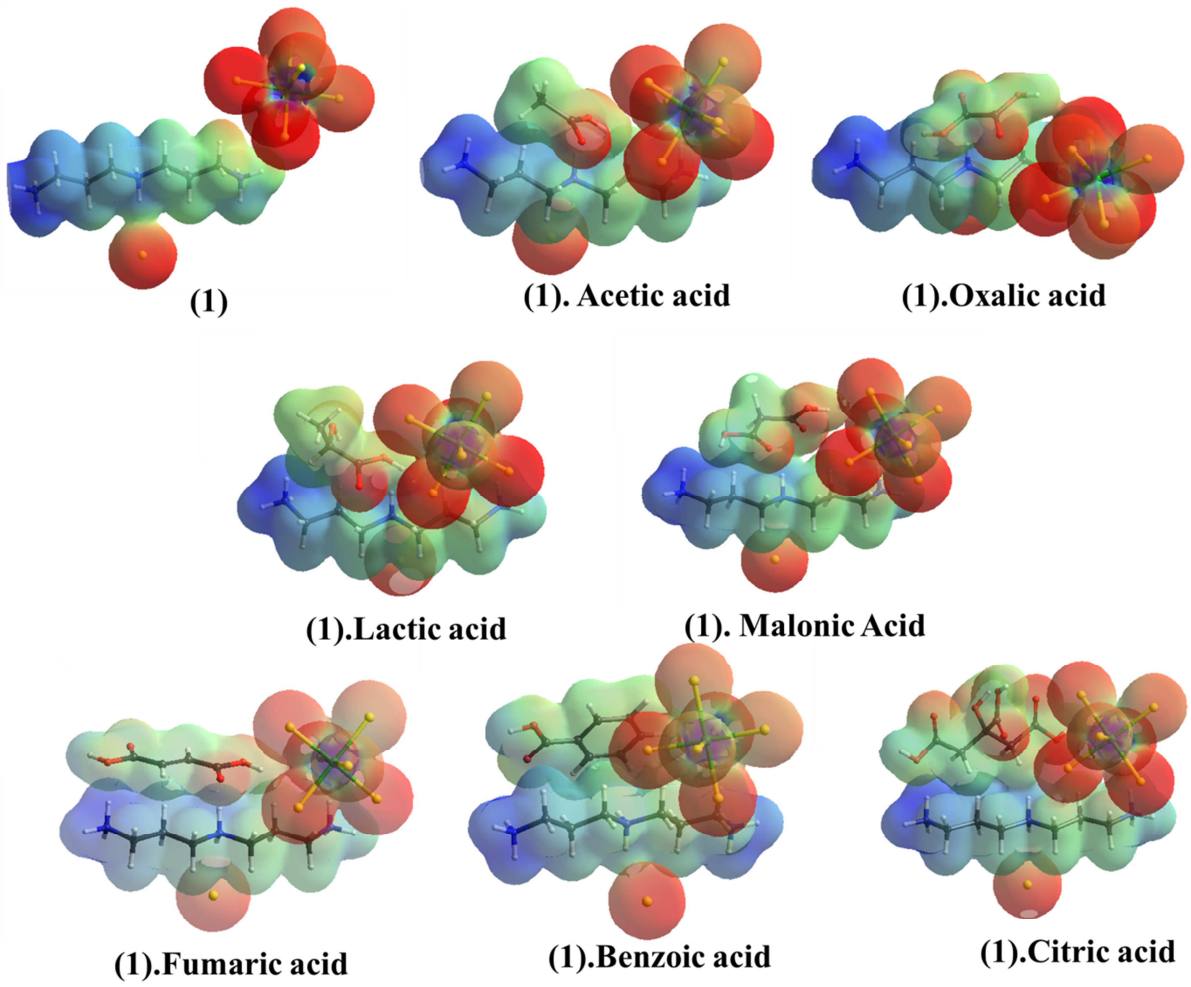

Figure 7. Electrostatic potential maps (-666—866 kJmol^{-1}) of **1** with organic acids

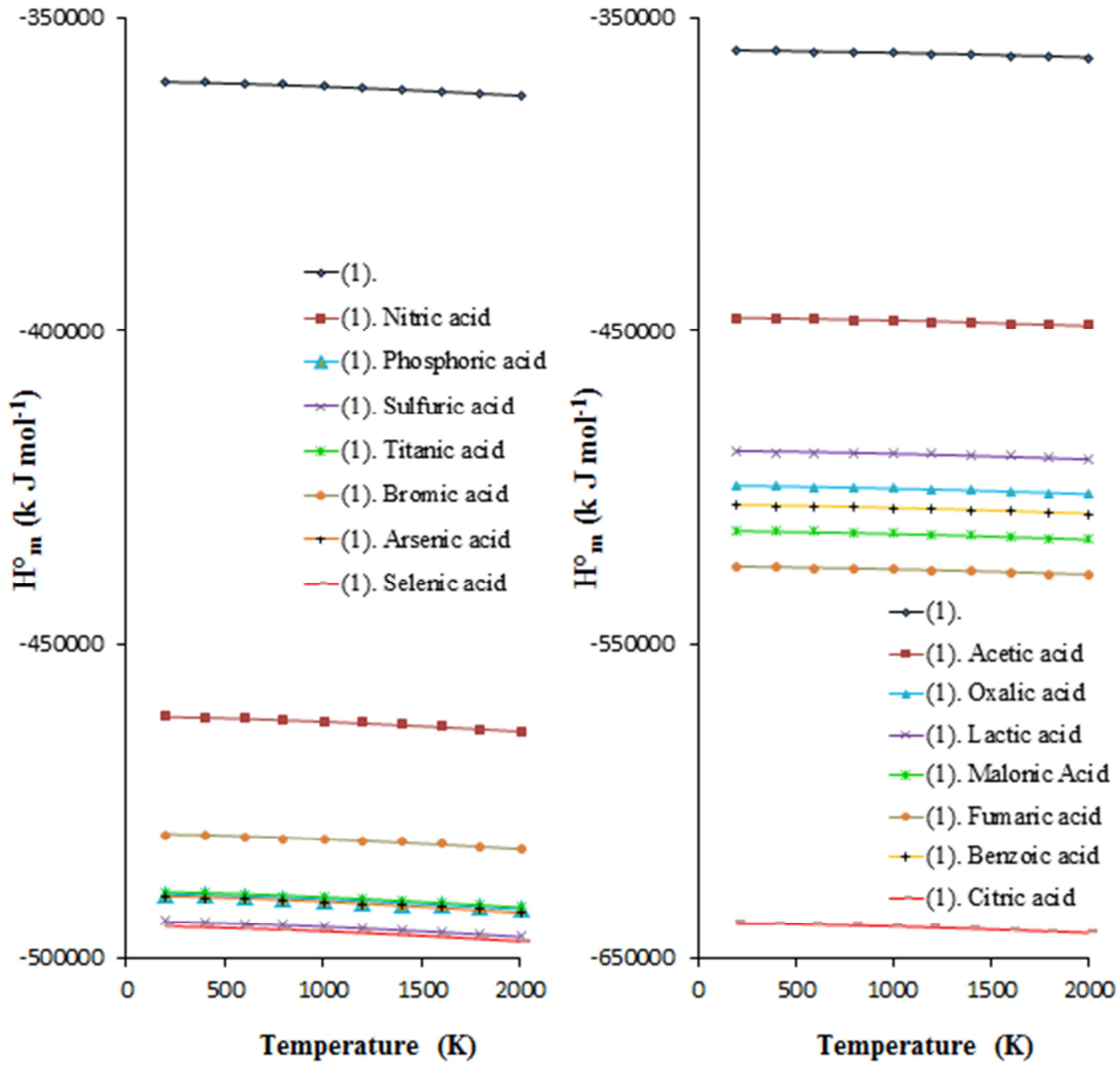

Figure 8. Variation of the enthalpy (H^o) with temperature for **1** and their derivatives

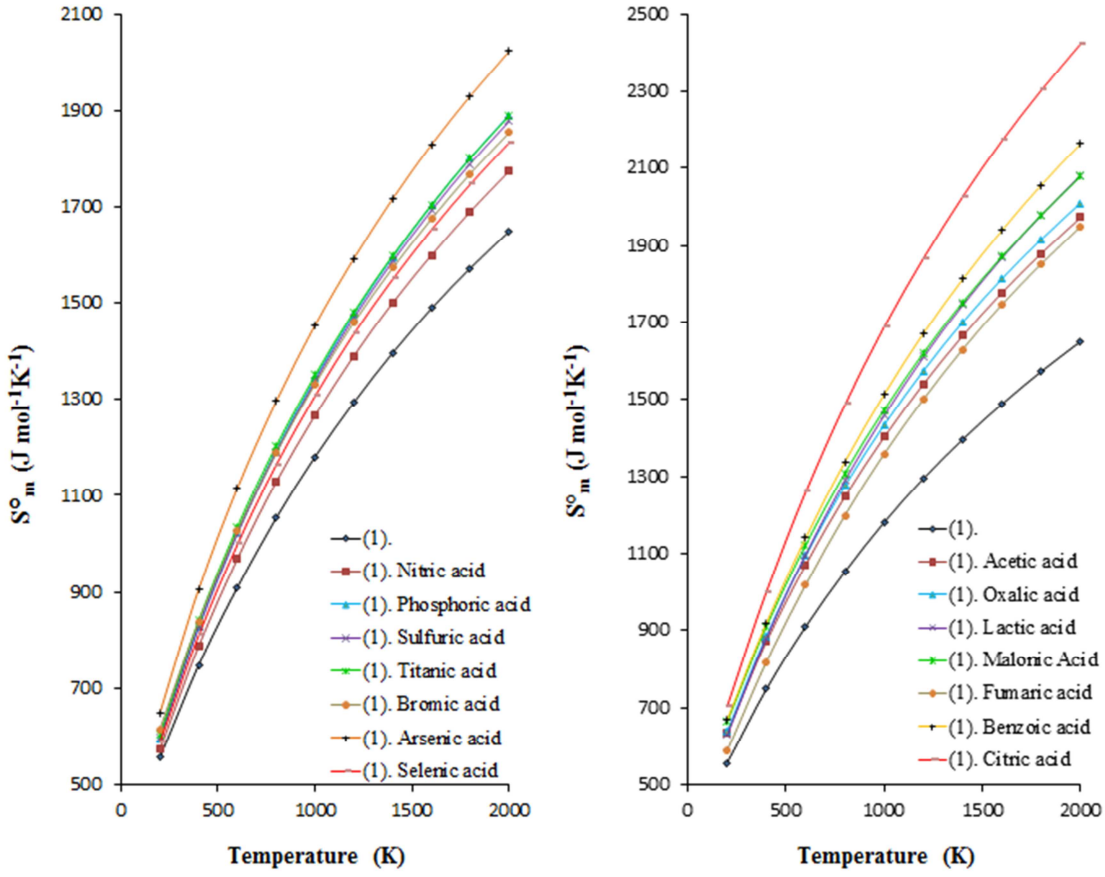

Figure 9. Variation of the entropy (S^o) with temperature for **1** and their derivatives

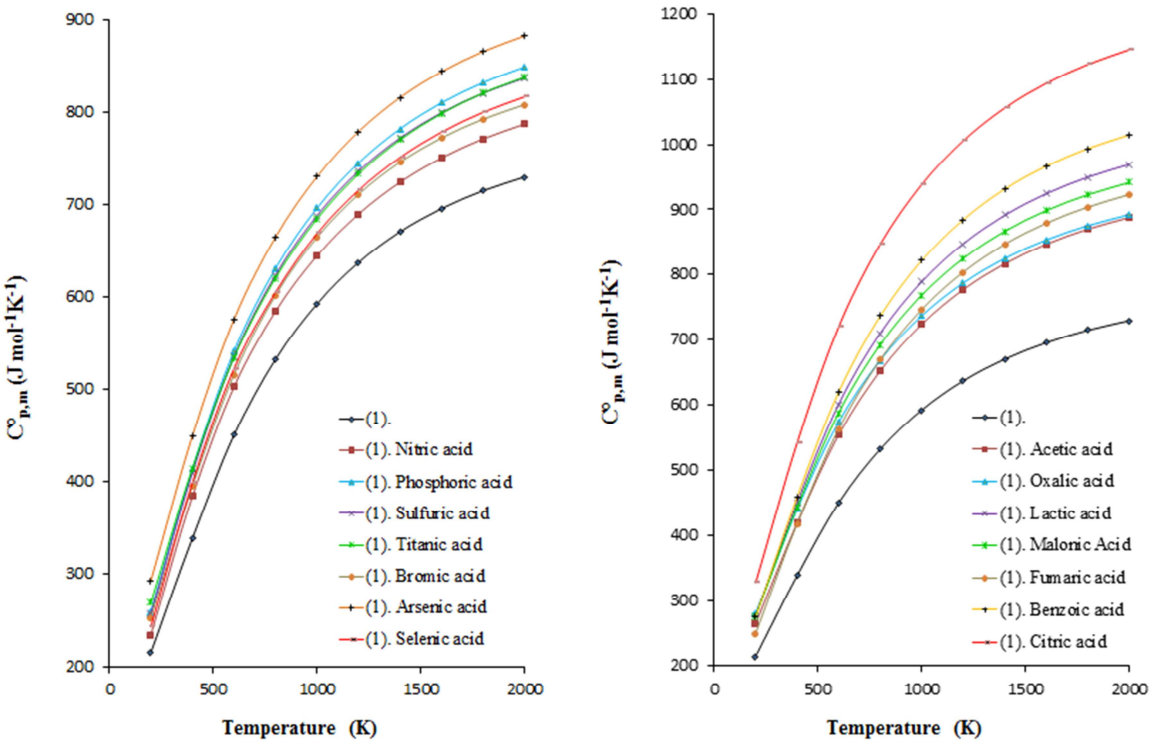

Figure 10. Variation of the heat capacity (C^{o}) with temperature for **1** and their derivatives

- Synthesis of a novel organo-chlorocadmate complex $(C_6H_{20}N_3)_2[Cd_2Cl_{10}]$
- Crystal structure study of the new compound
- Theoretical approach of $(C_6H_{20}N_3)_2[Cd_2Cl_{10}]$